Relativistic calculation of magnetic linear response functions using the Korringa–Kohn–Rostoker Green's function method

2001 J. Phys.: Condens. Matter 13 8551

(http://iopscience.iop.org/0953-8984/13/38/302)

INSTITUTE OF PHYSICS PUBLISHING JOURNAL OF PHYSICS: CONDENSED MATTER

J. Phys.: Condens. Matter **13** (2001) 8551–8564 PII: S0953-8984(01)24869-3

Relativistic calculation of magnetic linear response functions using the Korringa–Kohn–Rostoker Green's function method

M Deng, H Freyer, J Voitländer and H Ebert

University of Munich, Physical Chemistry, Butenandtstrasse 5-13, D-81377 München, Germany

Received 16 May 2001
Published 7 September 2001
Online at stacks.iop.org/JPhysCM/13/8551

Abstract

The relativistic KKR (Korringa–Kohn–Rostoker) Green's function method of band-structure calculation supplies an extremely flexible basis for calculating magnetic linear response functions of solids. An important feature of this approach is that it accounts properly for the influence of all relativistic effects. A brief introduction to this formalism is presented, together with some recent extensions to it. In particular, the inclusion of the orbital magnetization density induced by an external magnetic field allows a direct comparison with experiment for many different properties. This is demonstrated for the induced magnetic form factor, the magnetic susceptibility and the Knight shift of transition metals. A further appealing feature of the KKR formalism is that it is applicable in principle to any complex system. This property is exemplified by applications for the disordered alloy systems Ag_xPd_{1-x} and Ag_xPt_{1-x} that are treated with the help of the coherent potential approximation alloy theory.

1. Introduction

The use of the KKR (Korringa–Kohn–Rostoker) Green's function method to calculate magnetic linear response functions—for example, the magnetic susceptibility—was first suggested nearly 20 years ago [1]. In particular, the occurrence of inter-site effects on the Knight shift [2] has been discussed on that basis. Also the extension of the formalism to include relativistic effects has been worked out in the past [3], but the first applications became possible only a few years ago [4]. Recently, several important extensions of this very flexible approach were introduced [5, 6]: in calculating the Stoner enhancement of the Pauli spin susceptibility, the induced magnetization distribution is calculated self-consistently. In addition, the so-called Van Vleck orbital susceptibility [7] is calculated in a relativistic way using the KKR formalism. As a new feature of such calculations, a Stoner-like enhancement of the orbital susceptibility is accounted for by making use of the Brooks orbital polarization (OP) scheme [8, 9].

The calculation of the induced spin and orbital magnetization gives access to many interesting magnetic response functions—for example, the induced magnetic form factor.

Application of the KKR formalism in connection with the coherent potential approximation (CPA) alloy theory to disordered alloy systems seems to be especially interesting, because susceptibility and Knight shift measurements have often been used in the past to monitor the changes in the electronic structure of transition metals upon alloying. In particular, the alloy system Ag_xPd_{1-x} has been seen in the past as a prototype for a system behaving according to the rigid-band model [10]. Indeed, experimental data on the magnetic susceptibility [11] or the electronic specific heat [12], that represent the electronic structure in a global way, seemed to support this point of view. However, experiments that give information on the electronic structure in a component-resolved way—for example, ones based on the nuclear spin–lattice relaxation rate [2, 13]—cast doubt on this. Unfortunately, in the case of Ag_xPd_{1-x}, only Ag is easily accessible by means of NMR, while the Pd NMR became detectable only recently for Pd-rich Ag_xPd_{1-x} alloys [14]. For this reason, the isoelectronic system Ag_xPt_{1-x} was seen as a very attractive alternative, that allows NMR investigations on both alloy partners [15–17].

Because relativistic effects have a pronounced influence on NMR properties even for relatively light elements and because of the high atomic number of Pt, the use of the fully relativistic version of the KKR-CPA formalism seems to be indispensable for dealing with the alloy system Ag_xPt_{1-x}. Corresponding results for the magnetic susceptibility and the Knight shift for the two isoelectronic alloy systems Ag_xPd_{1-x} and Ag_xPt_{1-x} will be presented in the following and discussed in comparison with experimental data.

2. Theoretical framework

Within the relativistic KKR band-structure method used here, the electronic ground state of a paramagnetic solid is represented by the corresponding Green's function $G(\vec{r}, \vec{r}', E)$ [18]:

$$G(\vec{r}, \vec{r}', E) = \sum_{\Lambda\Lambda'} Z^n_\Lambda(\vec{r}, E)\tau^{nn'}_{\Lambda\Lambda'}(E)Z^{n'\times}_{\Lambda'}(\vec{r}', E) - \sum_{\Lambda}\left[Z^n_\Lambda(\vec{r}, E)J^{n\times}_\Lambda(\vec{r}', E)\Theta(r' - r) + J^n_\Lambda(\vec{r}, E)Z^{n\times}_\Lambda(\vec{r}', E)\Theta(r - r')\right]\delta_{nn'} \quad (1)$$

for $\vec{r}$ ($\vec{r}'$) within the atomic cell n (n'). Here the quantity $\tau^{nn'}_{\Lambda\Lambda'}(E)$ is the so-called scattering path operator [19] that represents all multiple-scattering events in a many-atom system in a consistent way (see below). The four-component wave functions Z^n_Λ and J^n_Λ are the properly normalized regular and irregular solutions of the corresponding single-site Dirac equation for site n. The appropriate relativistic spin–orbit and magnetic quantum numbers κ and μ, respectively, have been combined into $\Lambda = (\kappa, \mu)$ [20]. Finally, the superscript $\times$ in equation (1) indicates transposition together with complex conjugation restricted to the spin-angular part of the wave functions.

This platform allows one to deal with a distortion of the system due to an external magnetic field by using the Dyson equation

$$G^B = G + G\,\Delta\mathcal{H}\,G. \quad (2)$$

Here we restricted the modification of G to first order with respect to the perturbation Hamiltonian $\Delta\mathcal{H}$; that means a linear response is assumed. In the simplest approach, the Hamiltonian $\Delta\mathcal{H}$ represents a coupling only to the spin of the electrons [3]:

$$\Delta\mathcal{H}_{\rm spin}(\vec{r}) = \Delta\mathcal{H}^B_{\rm spin} + \Delta\mathcal{H}^{\rm xc}_{\rm spin}(\vec{r}). \quad (3)$$

That is,

$$\Delta\mathcal{H}_{\rm spin}(\vec{r}) = \beta\sigma_z\mu_{\rm B}B_{\rm ext} + \beta\sigma_z K^{{\rm xc},n}_{\rm spin}(\vec{r})\gamma^n(\vec{r})\chi^n_{\rm spin}\mu_{\rm B}B_{\rm ext} \quad (4)$$

where β is one of the standard Dirac matrices and σ_z is the z-component of the spin operator [20]. The first term in this expression is the conventional Zeeman term, while the second

one takes it into account that, because of the spin magnetization induced by the external magnetic field B_{ext}, the exchange correlation potential $V_{\mathrm{xc}}(\vec{r})$ will change. In equation (4) we made the usual assumption that this term depends linearly on the induced spin magnetization $m_{\mathrm{spin}}(\vec{r})$ with the corresponding interaction kernel $K^{\mathrm{xc},n}_{\mathrm{spin}}(\vec{r})$ [21]. For $\vec{r}$ within the atomic cell n, $m_{\mathrm{spin}}(\vec{r})$ in turn can be replaced by the product $\gamma^n(\vec{r})\chi^n_{\mathrm{spin}}B_{\mathrm{ext}}$ with $\gamma^n(\vec{r})$ the normalized spin density and χ^n_{spin} the local spin susceptibility for site n. Usually, $\gamma^n(\vec{r})$ is approximated by the average over the square of the wave functions $|\psi(E_{\mathrm{F}})|^2$ at the Fermi level.

Using G^B as given in equation (2) together with equation (4) to calculate the induced spin magnetization $m^n_{\mathrm{spin}}(\vec{r})$ for an atomic site n, one now arrives at

$$m^n_{\mathrm{spin}}(\vec{r}) = -\frac{\mu_{\mathrm{B}}}{\pi}\Im\int^{E_{\mathrm{F}}}\mathrm{d}E\sum_{n'}\int_{\Omega_{\mathrm{WS}_{n'}}}\mathrm{d}^3r'\,\beta\sigma_z G(\vec{r},\vec{r}',E) \times\left(\beta\sigma_z+\beta\sigma_z K^{\mathrm{xc},n}_{\mathrm{spin}}(\vec{r}')\gamma^{n'}(\vec{r}')\chi^{n'}_{\mathrm{spin}}\right)B_{\mathrm{ext}}G(\vec{r}',\vec{r},E) \tag{5}$$

where $\vec{r}'$ is restricted to the atomic cell n'. For a pure system the corresponding Pauli spin susceptibility χ^n_{spin} does not depend on the site n and one gets the conventional expression for the Stoner-enhanced Pauli spin susceptibility χ^n_{spin}:

$$\chi_{\mathrm{spin}} = S\chi^0_{\mathrm{spin}}. \tag{6}$$

Here S is the so-called Stoner enhancement factor, that is usually written as $(1 - I\chi^0_{\mathrm{spin}})^{-1}$, with I the Stoner exchange–correlation integral [21] and χ^0_{spin} the unenhanced Pauli spin susceptibility that is obtained if the second term in equation (4) is ignored. For more complex systems with more than one atom type, equation (5) leads to a system of linear equations for the local susceptibilities χ^n_{spin}. As a consequence, the Stoner enhancement factor will also depend on the lattice site or atom type.

The Hamiltonian in equation (3) accounts only for the coupling of the external magnetic field to the electronic spin. Within a non-relativistic theory, the coupling to the orbital degree of freedom leads, in addition to the spin susceptibility, to the Langevin and Landau diamagnetic as well as to the Van Vleck paramagnetic susceptibility [2, 7]. The Langevin diamagnetic susceptibility χ_{dia} can be calculated straightforwardly in a relativistic manner [22]. This applies also for the Van Vleck susceptibility χ_{VV} that is derived from the expectation value of the z-component of the orbital angular momentum operator l_z and using the perturbation Hamiltonian [5, 6]:

$$\Delta\mathcal{H}_{\mathrm{orb}} = \beta l_z B_{\mathrm{ext}}. \tag{7}$$

Calculating χ_{VV} within the framework of plain spin-density functional theory (SDFT), there is no modification of the electronic potential due to the induced orbital magnetization. Working instead within the more appropriate current-density functional theory, however, there would be a correction to the exchange–correlation potential just as in the case of the spin susceptibility giving rise to a Stoner-like enhancement. Alternatively, this effect can be accounted for by adopting the Brooks orbital polarization (OP) formalism [8, 9]. This leads to expressions for the enhanced Van Vleck susceptibility χ_{VV} completely analogous to equations (3)–(5).

Within a non-relativistic formalism the spin and orbital degrees of freedom are completely decoupled; this means that the cross-terms $\langle\sigma_z G l_z G\rangle$ and $\langle l_z G\sigma_z G\rangle$ vanish. However, Yasui and Shimizu [23], who used a rather different theoretical approach to deal with the magnetic susceptibility of transition metals, pointed out that these cross-terms do not vanish if the spin–orbit coupling is present. However, these cross-terms, denoted as χ_{SO} and χ_{OS}, respectively, in the following, turn out to be much smaller than χ_{P} or χ_{VV}.

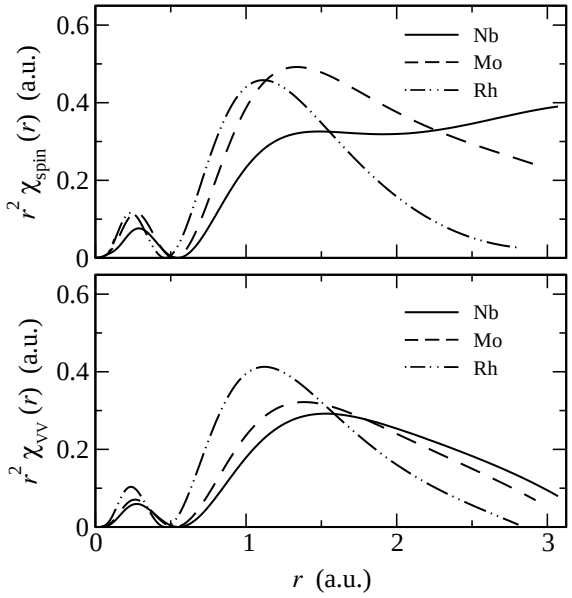

Figure 1. Spherically averaged spin and Van Vleck r-dependent susceptibilities $\chi_{\rm spin}(r)$ and $\chi_{\rm VV}(r)$, respectively, weighted with r^2 for Nb, Mo and Rh.

The remaining diamagnetic Landau susceptibility $\chi_{\rm L}$ is normally assumed to be small compared to all the other contributions. In addition, it is rather cumbersome to calculate [7]. For these reasons it has not been considered here (see below).

The relativistic KKR formalism sketched here has been employed by Staunton and co-workers to calculate the spin susceptibility of the pure elements Co, Sc and Y [4, 24] using the approximation for the normalized spin $\gamma(\vec{r})$ mentioned above. Here we apply this approach to binary disordered alloys making use of the CPA alloy theory. For this purpose one has to deal with the configurational average for expressions of the type $\langle\hat{A}G\hat{B}G\rangle$, with $\hat{A}$ and $\hat{B}$ being arbitrary operators. The conceptual problems connected with this average within the framework of the KKR-CPA were first discussed by Staunton [3] for the case of spin susceptibility, which means for $\hat{A} = \hat{B} = \beta\sigma_z$ on the basis of the work of Durham *et al* [25]. A very detailed investigation was made later by Butler [26] who studied the problem in the context of the electronic conductivity for which $\hat{A} = \hat{B} = \vec{j}$ is the current-density operator. For the applications to be presented below, it turned out that using the approximation $\langle\hat{A}G\rangle\langle\hat{B}G\rangle$ is well justified, which means that the vertex corrections defined as $\langle\hat{A}G\hat{B}G\rangle - \langle\hat{A}G\rangle\langle\hat{B}G\rangle$ could be ignored.

3. Induced magnetization and form factor

Initially the formalism presented above was primarily meant to calculate the spin susceptibility $\chi_{\rm spin}$. However, equation (5) shows that the primary quantity to be considered is the induced spin magnetization $m_{\rm spin}(\vec{r})$. In the top panel of figure 1 corresponding results for $m_{\rm spin}(\vec{r})$ are shown for Nb, Mo and Rh in terms of the r-dependent susceptibility $\chi_{\rm spin}(r) = \gamma(\vec{r})\chi_{\rm spin}$. As mentioned above, the normalized spin density $\gamma(\vec{r})$ is in general approximated by averaging the square of the wave functions at the Fermi level. This approximation can be used as an initial guess for an iterative calculation of the true r-dependence of $\gamma(\vec{r})$ on the basis of equation (5).

Although this procedure leads only to minor modifications to $\gamma(\vec{r})$, these can lead to quite important corrections for the Stoner enhancement of $\chi_{\rm spin}$.

Completely analogously to the induced spin magnetization $m_{\rm spin}(\vec{r})$, one may introduce the induced orbital magnetization $m_{\rm orb}(\vec{r})$ corresponding to the operator $\mu_{\rm B}\beta l_z$. For Nb, Mo and Rh the calculated $m_{\rm orb}(\vec{r})$ is given in the lower panel of figure 1 in terms of the corresponding r-dependent Van Vleck susceptibility $\chi_{\rm VV}(r)$. As one notes, $\chi_{\rm VV}(r)$ differs in general in a rather pronounced way from its spin counterpart. The reason for this is that $\chi_{\rm spin}(r)$ is determined primarily by states at the Fermi level, while all states of the occupied part of the valence band contribute to $\chi_{\rm VV}(r)$.

With the induced spin and orbital magnetization available, one immediately gets access to the corresponding induced magnetic form factors $f_{\rm spin}(\vec{q})$ and $f_{\rm orb}(\vec{q})$, respectively. Adopting the conventional approach [27], these induced form factors can be obtained as functions of the scattering vector $\vec{q}$ from the expressions

$$f_{\rm spin}(\vec{q}) = \frac{1}{\mu_{\rm spin}} \int_{\Omega_{\rm WS}} {\rm d}^3 r \; j_0(\vec{q}\,.\,\vec{r}) m_{\rm spin}(\vec{r}) \tag{8}$$

$$f_{\rm orb}(\vec{q}) = \frac{1}{\mu_{\rm orb}} \int_{\Omega_{\rm WS}} {\rm d}^3 r \; (j_0(\vec{q}\,.\,\vec{r}) + j_2(\vec{q}\,.\,\vec{r})) m_{\rm orb}(\vec{r}). \tag{9}$$

These can be directly compared with experimental data stemming from elastic neutron scattering experiments by taking the appropriate average:

$$\bar{f}(\vec{q}) = \frac{f_{\rm spin}(\vec{q})\chi_{\rm spin} + f_{\rm orb}(\vec{q})\chi_{\rm VV}}{\chi_{\rm spin} + \chi_{\rm VV}} \tag{10}$$

if the small additional contribution to the experimental form factor corresponding to the Langevin diamagnetic susceptibility $\chi_{\rm dia}$ is accounted for. Figure 2 shows the resulting theoretical induced magnetic form factor $\bar{f}$ for V and Cr in comparison with experimental data. The difference between the spatial distributions of the induced spin and orbital magnetization seen in figure 1 is obviously reflected by different dependences of the corresponding induced magnetic form factors on the scattering vector $\vec{q}$. This implies in particular that comparison with experiment supplies a rather severe check for the relative magnitude of the calculated spin and orbital susceptibilities $\chi_{\rm spin}$ and $\chi_{\rm VV}$. As can be seen from figure 2 this is quite different for V and Cr and found to be in excellent agreement with experiment.

4. Magnetic susceptibility

Most susceptibility and NMR measurements on Ag_xPd_{1-x} and Ag_xPt_{1-x} were done in the past to obtain information on the electronic structure of these isoelectronic alloy systems. The most prominent feature of the electronic band structure of the common alloy partner Ag is its rather narrow d band that has a width of only 3.1 eV and lies about 3.2 eV below the Fermi level. Pd or Pt, on the other hand, have d bandwidths of about 7.4 eV with the Fermi level cutting the d-band complex. As a consequence of the rather different properties of these elements, alloy formation has a rather strong impact on their electronic structure.

Like the previous calculations on Ag_xPd_{1-x} by Pindor *et al* [31] and Winter and Stocks [32] and on Ag_xPt_{1-x} by Ebert *et al* [33], the present calculations give a split-band structure with separate Ag and Pd (Pt) bands for all concentrations. The high-energy hump arises from Pd (Pt) and the low-energy one is due to the Ag. In addition, one finds that the bandwidth of Ag in Ag_xPd_{1-x} gets larger with increasing Ag content, while that of Pd decreases at the same time. A similar behaviour is found for Ag_xPt_{1-x}.

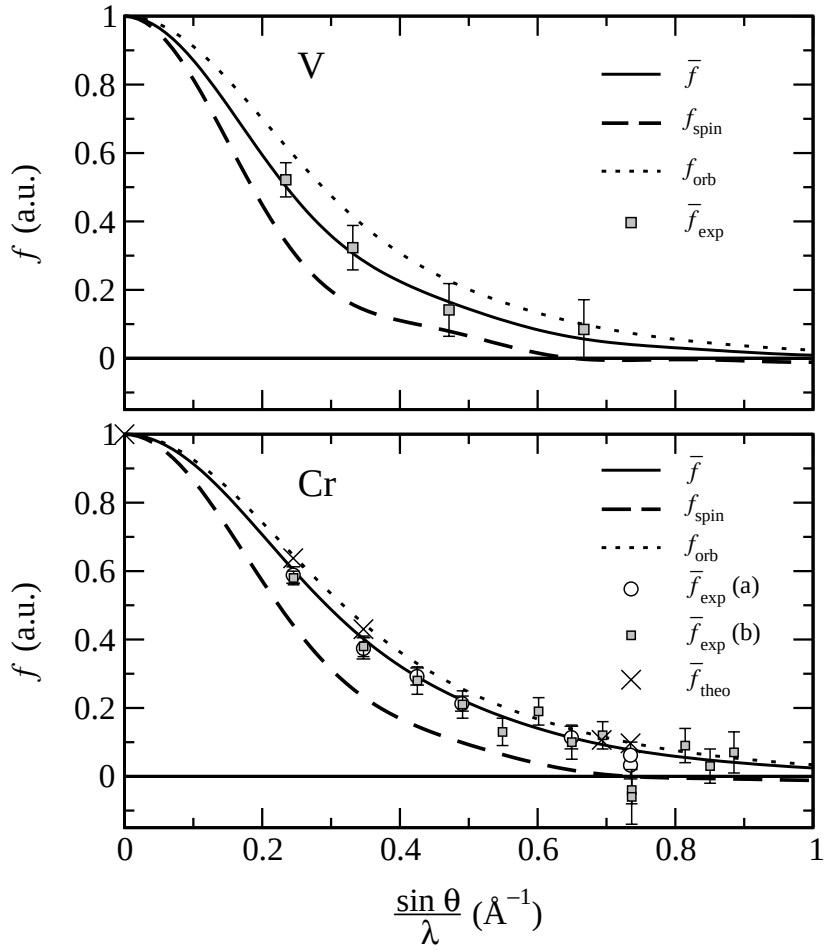

Figure 2. The theoretical induced magnetic form factor $\bar{f}$ for the transition metals V and Cr together with corresponding experimental data (V: [28]; Cr: [29]). For Cr, theoretical data obtained by Oh *et al* [30] have been added.

Since the Ag d band is located much lower in energy than that for Pd (Pt), the Ag d band remains fully occupied, when Ag is alloyed with Pd (Pt). As a consequence, the density of states (DOS) at the Fermi energy is dominated by the Pd (Pt) d states for most concentrations. The increase in Ag content leads to a shift of the Pd (Pt) bands towards lower energies. This gives rise to a monotonic and rapid decrease of the DOS at E_F with the filling of the Pd (Pt) d bands as can be seen in figure 3.

This feature is reflected by many different physical properties—for example, the electronic specific heat coefficient γ [12]. In the past it has been assumed that the magnetic susceptibility χ should also directly reflect the DOS at the Fermi level [11]. In particular, the rapid decrease of χ of Pd when Ag is added has been interpreted in the spirit of the rigid-band model to be a consequence of the filling of the Pd d band with the additional Ag valence electrons. The following investigations will show that this point of view is oversimplified for many different reasons.

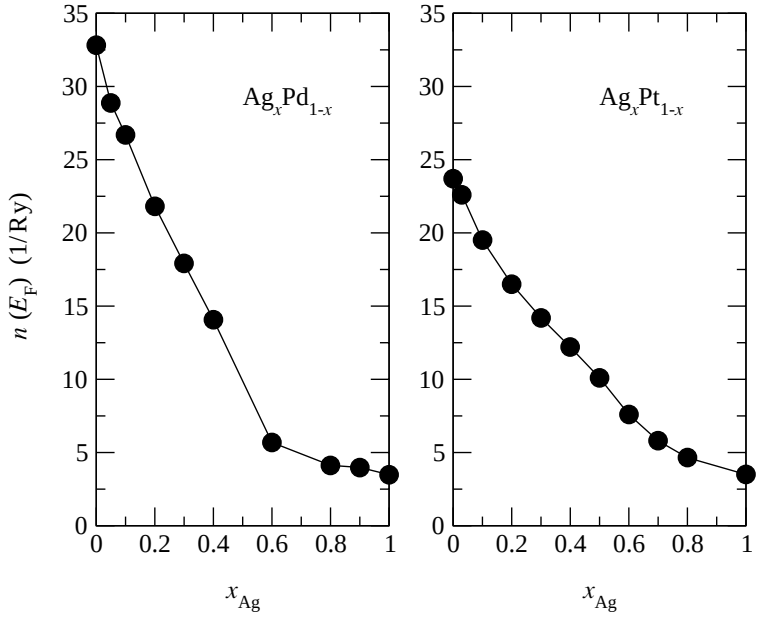

Figure 3. Calculated total densities of states at the Fermi energy for Ag_xPd_{1-x} and Ag_xPt_{1-x} as functions of the Ag concentration.

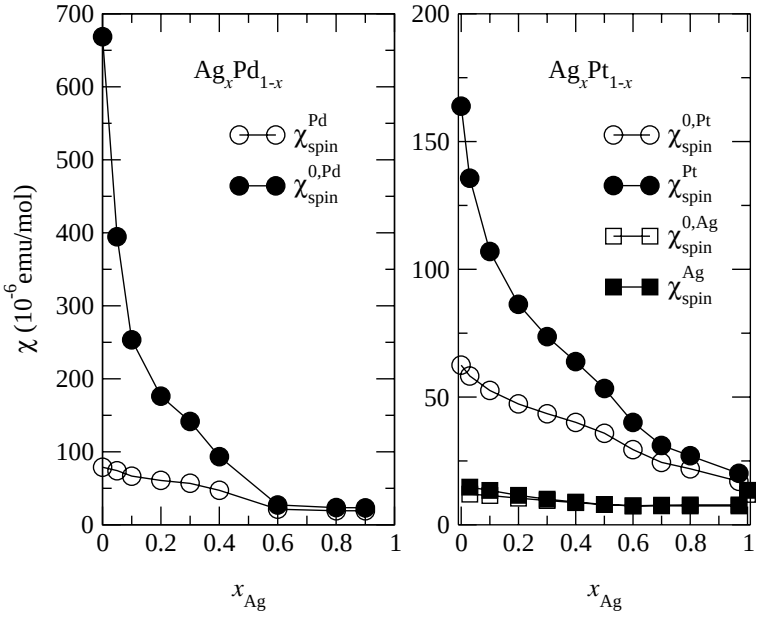

Figure 4. Calculated component-resolved Pauli spin contributions to the magnetic susceptibilities of Ag_xPd_{1-x} and Ag_xPd_{1-x} as functions of the Ag concentration. The Pauli spin susceptibilities are given without Stoner enhancement, $\chi^{0,\alpha}_{spin}$, and with Stoner enhancement, χ^{α}_{spin}.

The calculated results for the Pauli contributions to the magnetic susceptibility of the various alloy partners in Ag_xPd_{1-x} and Ag_xPt_{1-x} are shown in figure 4. As expected from

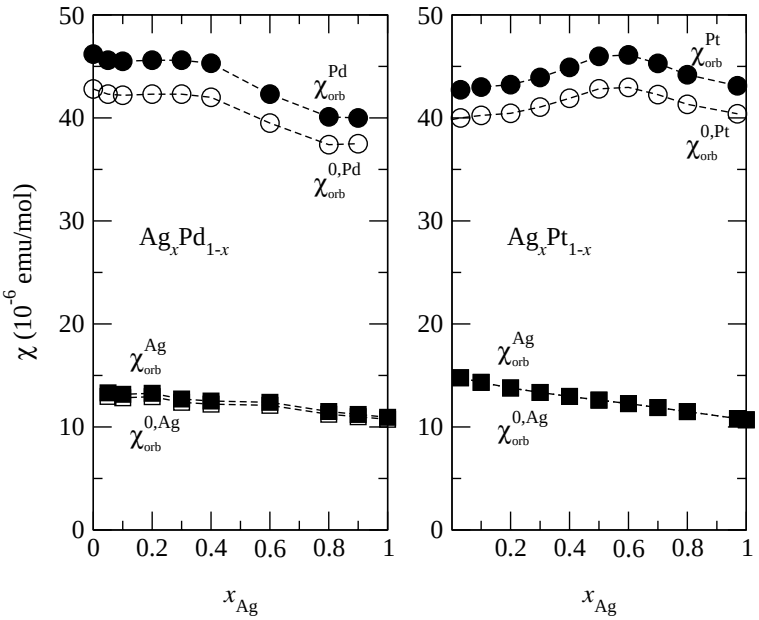

Figure 5. Calculated component-resolved Van Vleck orbital contributions to the magnetic susceptibilities for Ag_xPd_{1-x} and Ag_xPt_{1-x} as functions of the Ag concentration. The Van Vleck susceptibilities are given without OP enhancement, $\chi_{VV}^{0,\alpha}$, and with OP enhancement, χ_{VV}^{α}.

the behaviour of the partial DOS for these two alloy systems, the relatively high unenhanced Pauli susceptibilities $\chi_{spin}^{0,Pd}$ and $\chi_{spin}^{0,Pt}$ of pure Pd and Pt, respectively, decrease rapidly with increasing Ag content. The partial susceptibility $\chi_{spin}^{0,Ag}$ of Ag, on the other hand, is rather small and hardly varies with concentration for both alloy systems. Because $\chi_{spin}^{0,Ag}$ for Ag_xPd_{1-x} is much smaller than $\chi_{spin}^{0,Pd}$ and because it is very similar to $\chi_{spin}^{0,Ag}$ for Ag_xPt_{1-x}, it has been omitted on the left side of figure 4.

As one can see from figure 4, the Stoner enhancements of the Pauli spin susceptibilities for pure Pd and Pt are rather large. Accordingly, these elements completely dominate the total magnetic susceptibility on the Ag-poor side for the two alloy systems. Because the Stoner enhancement also gets weaker when the spin susceptibility χ_{spin}^{0} decreases, the partial susceptibilities of Pd and Pt decrease more rapidly with increasing x than the bare density of states at the Fermi level shown in figure 3 suggests.

For the alloy partner Ag, on the other hand, the situations are quite different in the two alloy systems. Here the Stoner enhancement amounts to only some few per cent. Only on the Ag-poor side is it somewhat more pronounced. On the Ag-rich side, however, it can more or less be ignored. Again χ_{spin}^{Ag} for Ag in Ag_xPd_{1-x} has been omitted in the left part of figure 4 for the reasons given above.

In figure 5, the Van Vleck contributions without and with the OP enhancement, $\chi_{VV}^{0,\alpha}$ and χ_{VV}^{α}, respectively, to the magnetic susceptibilities of each component in the two alloy systems are shown. The concentration dependency of χ_{VV}^{α} is obviously very different from that of χ_{spin}^{α} because χ_{VV}^{α} is primarily determined by the filling and width of the d band, while χ_{spin}^{α} is connected with the DOS at the Fermi level. As can be seen in the figure 5, χ_{VV}^{Pd} reduces continuously due to the relatively strong variation in the filling of the d band of Ag_xPd_{1-x}

upon increasing the Ag content x. χ_{VV}^{Pt} for Pt in Ag_xPt_{1-x}, on the other hand, shows a weak maximum around $x = 0.6$. On the Ag-poor side, χ_{VV}^{Pd} in Ag_xPd_{1-x} is similar in magnitude to χ_{VV}^{Pt} in Ag_xPt_{1-x}. However, for large Ag concentrations, χ_{VV}^{Pt} is found to be larger than χ_{VV}^{Pd}. The increases of the Van Vleck susceptibilities ($\chi_{VV}^{\alpha} - \chi_{VV}^{0,\alpha}$) due to the OP mechanism are nearly the same for Pd and Pt. In the two cases, they amount to around 4×10^{-6} emu mol^{-1}. The results for χ_{VV}^{Ag} for the two alloys are very similar, showing a slight decrease with increasing concentration x. In contrast to the case for Pd and Pt, the OP enhancement contributes a negligibly small amount to χ_{VV}^{Ag} for both alloys.

The negative Langevin susceptibility χ_{dia}^{α}, for all components, was found to hardly vary with concentration x. It more or less compensates for the positive orbital contribution χ_{VV}^{α} of the corresponding atom. A variation in χ_{dia}^{α} with concentration should primarily arise from the change of the lattice parameter with concentration [34]. It seems that this effect is not very pronounced for the alloys under investigation.

In accordance with the strong relativistic effects that can be expected for Pt in Ag_xPd_{1-x}, the spin–orbit cross-term contributions χ_{SO}^{Pt} and χ_{OS}^{Pt} (not shown here), which are almost of the same magnitude, should not be ignored over the whole concentration range. For Pd in Ag_xPd_{1-x}, the corresponding contributions are of the same order on the Ag-poor side as for Pt in Ag_xPd_{1-x}, but they are very small on the Ag-rich side. For both alloy systems the cross-term contributions of Ag can be ignored over the entire composition range.

The magnetic susceptibility of the system Ag_xPd_{1-x} has been measured by several authors at various temperatures [11, 13, 35]. The experimental data show that the magnetic susceptibility of this system depends strongly on temperature but becomes almost independent of temperature for $x > 0.6$ (see figure 6). This implies in particular that the strongly temperature-dependent Pauli susceptibility of Pd contributes dominantly to the total magnetic susceptibility on the Ag-poor side of Ag_xPd_{1-x}. However, with the rapid diminishing of the Pauli susceptibility of Pd with increasing x, the other contributions of Pd and the contributions of Ag, which are only slightly temperature dependent, become more and more important.

In figure 6, the calculated partial susceptibility $\chi^{\alpha} = \chi_{spin}^{\alpha} + \chi_{VV}^{\alpha} + \chi_{SO}^{\alpha} + \chi_{OS}^{\alpha} + \chi_{dia}^{\alpha}$ as well as the total susceptibility $\chi = \sum_{\alpha} x_{\alpha} \chi^{\alpha}$ for the alloy systems Ag_xPd_{1-x} and Ag_xPt_{1-x} are shown together with the corresponding experimental data [13, 16, 35]. For pure Pd, the calculated total magnetic susceptibility is found to be in very good agreement with the value measured at 4 K [36]. Keeping in mind that the Landau susceptibility term χ_{L}^{α} has been ignored, one can say that the corresponding experimental data for Ag_xPd_{1-x} are fairly well reproduced by the calculations over the entire concentration range.

Because the fcc metals Ag and Pt form a peritectic system and therefore have only limited solid solubility, metastable single-phase crystalline Ag_xPt_{1-x} alloys had to be prepared by rapid quenching from the melt. This allowed us to perform experimental investigations of the magnetic and NMR properties of this alloy system over the whole range of concentrations [16]. As for Ag_xPd_{1-x}, figure 6 demonstrates that the susceptibilities calculated within this work reproduce the experimental data for the alloy system Ag_xPt_{1-x} measured at 4.2 K [16] very well.

5. Knight shift

It was found in many experimental investigations that the Knight shifts of the noble metals Au, Ag and Cu are positive but become negative if they are dissolved as impurities in the transition metals Pd and Pt [2, 13, 16, 37–39]. It was assumed already by Kobayashi *et al* [37] that the negative Knight shifts of the noble metals in the corresponding alloys with Pd and

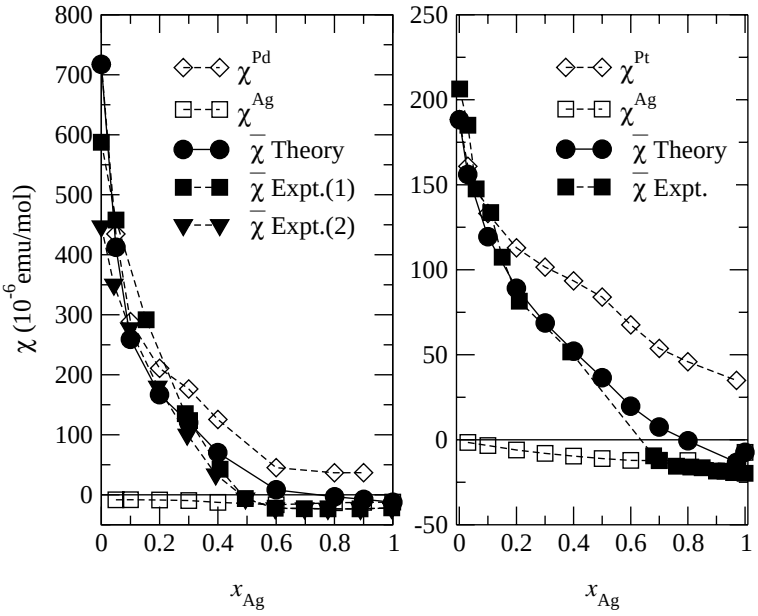

Figure 6. Calculated partial magnetic susceptibilities for Ag, Pd and Pt in Ag_xPd_{1-x} and Ag_xPt_{1-x}, as well as the total susceptibility as functions of the Ag concentration together with corresponding experimental data [13, 16, 35]. The experimental data for Ag_xPd_{1-x} marked 'Expt. (1)' and 'Expt. (2)' were measured at 291 K [35] and 421 K [13], respectively.

Pt are not due to the polarization of the core electrons, as in the case of pure Pd [40], but due to the influence of the host metals Pd and Pt stemming from their strongly enhanced spin susceptibility. The underlying mechanism giving rise to the observed negative Knight shift was always assumed to be essentially the same as that leading to the negative hyperfine field of the noble metals dissolved in a ferromagnetic host metal [2]. This assumption can now be verified in a quite straightforward way by the calculation of the spin contributions to the Knight shifts of each component in the alloy systems Ag_xPd_{1-x} and Ag_xPt_{1-x}. A non-relativistic formulation for the Knight shift in metals due to the Fermi contact interaction within the framework of the KKR formalism was already given by Gyorffy [41] nearly 30 years ago. The formalism sketched above allows a straightforward fully relativistic extension [5] using the expression

$$K = -\frac{e}{\pi B_{\rm ext}} \Im \int^{E_{\rm F}} {\rm d}E \; \frac{(\vec{r} \times \vec{\alpha})_z}{r^3} G^B(\vec{r}, \vec{r}, E) \tag{11}$$

where the observable in the integral corresponds to the vector potential stemming from the nuclear magnetic dipole moment [20]. Inserting the Green's function $G^B(\vec{r}, \vec{r}, E)$ according to equation (2), one notes that there are contributions to K because of the coupling of an external magnetic field to the spin ($\Delta\mathcal{H}_{\rm spin}$) as well as to the orbital degree of freedom ($\Delta\mathcal{H}_{\rm orb}$) of the electrons. Furthermore, one notes that the Stoner mechanism leads to an enhancement of the corresponding shift contributions as for the spin and orbital susceptibilities, $\chi_{\rm spin}$ and $\chi_{\rm VV}$, respectively.

The calculated valence band spin contributions to the Knight shifts without and with Stoner enhancement, $K^0_{\rm spin}$ and $K_{\rm spin}$, respectively, for each component in Ag_xPd_{1-x} and Ag_xPt_{1-x} are shown in figure 7. In addition, the contributions from the core polarization $K_{\rm cp}$ that correspond

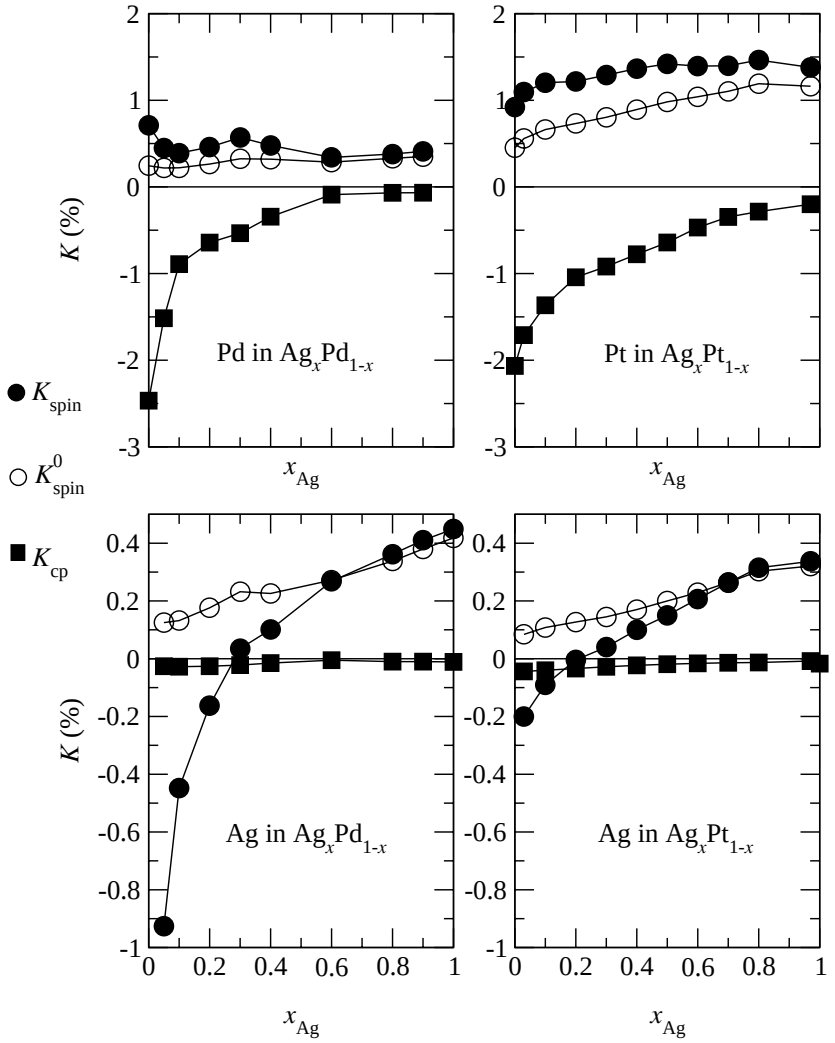

Figure 7. Calculated spin contributions without (K^0_{spin}) and with Stoner enhancement (K_{spin}) and the core polarization contribution (K_{cp}) to the Knight shifts of Ag, Pd and Pt in $\mathrm{Ag}_x\mathrm{Pd}_{1-x}$ and $\mathrm{Ag}_x\mathrm{Pt}_{1-x}$.

to the enhanced spin susceptibilities $\chi^{\alpha}_{\mathrm{spin}}$ are given. Due to the large spin magnetization of Pd and Pt on the Ag-poor side for both alloy systems, the contributions from the core polarization K_{cp} for Pd and Pt are very large. They decrease rapidly with increasing Ag concentration x and thus with decreasing spin magnetization, as shown in the top panel of figure 7. For Ag, on the other hand, the core polarization contributions are nearly zero in the two alloy systems, as can be seen in the lower panel of the figure. However, the Stoner-enhanced spin contribution to the Knight shift of Ag, for both alloys, has relatively large absolute value with a negative sign on the Ag-poor side, which is attributed to inter-atomic effects arising from the strong induced spin magnetization of the corresponding transition metal, Pd or Pt. This finding is completely in line with the results of our previous calculations [14, 42] that included the effect of an external magnetic field in the SCF cycle. The analysis of the induced spin density of

the various components in the alloys $Ag_{0.10}Pd_{0.90}$ and $Cu_{0.10}Pd_{0.90}$ demonstrated that for Pd the core polarization dominates the magnetization at the nuclear site. For Ag and Cu, on the other hand, the Stoner-enhanced spin density of the valence electrons has negative sign and is responsible for the main part in the magnetization at the nuclear site. Since the spin density at a nuclear site leads to the Fermi contact contributions to the Knight shift, it was concluded that the negative Knight shift of the noble metal arises from the large induced spin moment of neighbouring Pd atoms in the alloy, instead of from the much smaller magnetization within the atomic cell of Ag or Cu. Obviously, the calculated results shown in figure 7 are in full accordance with this interpretation.

As can be seen in figure 7, the unenhanced spin contribution $K^0_{\rm spin}$ to the Knight shift for each component in the two alloys shows a similar trend, i.e. it increases smoothly with increasing Ag concentration. This seems to be primarily due to the fact that the conventional Fermi contact contribution is included in $K^0_{\rm spin}$. Within a simplified approach [43], this contribution is proportional to the s-like density of states at the Fermi energy and the corresponding coupling constant or hyperfine field. Indeed, the s component of the DOS at $E_{\rm F}$ shows a smooth increase for each component with increasing Ag concentration, leading in this way to the corresponding increase of the contribution $K^0_{\rm spin}$.

In contrast to the case for most previous theoretical investigations on Knight shifts, the Van Vleck contribution was calculated as well. As for the corresponding contribution to the Van Vleck susceptibility $\chi_{\rm VV}$, the OP enhancement was also considered, in addition. As in the case of $\chi_{\rm VV}$, the orbital contributions to the Knight shifts of Pd and Pt do not change much over the entire concentration range and are much larger than those of Ag in both alloy systems. Due to the larger atomic number of Pt compared with that of Pd, $K^0_{\rm VV}$ as well as $K_{\rm VV}$ is larger for Pt than for Pd. For Ag the situation is again very similar for the two alloy systems. In particular, one finds, as for the corresponding Van Vleck susceptibility $\chi^{\rm Ag}_{\rm VV}$, that the OP enhancement is very small.

The diamagnetic contributions $K_{\rm dia}$ to the Knight shifts for each component in the two alloy systems hardly change over the entire concentration range. For Pt the absolute value of $K_{\rm dia}$ is about two times larger than for the other components in the alloy systems. For Pd as well as Pt, the orbital Van Vleck contributions $K_{\rm VV}$ are larger than the absolute values of the corresponding diamagnetic contributions $K_{\rm dia}$. For Ag, on the other hand, the situation is just the reverse.

The experimental Knight shifts of Ag and Pt in Ag_xPt_{1-x} could be determined by using samples rapidly quenched from the melt [16, 44]. Corresponding experimental data for Ag in Ag_xPd_{1-x} are also available [2]. Because the huge quadrupole moment of Pd gives rise to an extremely broad line resulting in a very weak NMR signal, it only became possible to detect the Pd NMR for Pd-rich Ag_xPd_{1-x} recently [14].

The calculated total Knight shifts $K_{\rm theory} = K_{\rm spin} + K_{\rm VV} + K_{\rm cp} + K_{\rm dia}$ for the various components in the alloy systems Ag_xPd_{1-x} and Ag_xPt_{1-x}, compared with the corresponding experimental data, are shown in figure 8. Obviously, the main features of the measured data are well reproduced by the theoretical results. The negative Knight shift of Pd has a larger absolute value than the corresponding one of Pt on the Ag-poor side for both alloy systems. This is mainly due to the stronger core polarization, which arises from the Stoner enhancement of the Pauli spin susceptibility. On the Ag-rich side, the Knight shift of Pt is somewhat larger than that of Pd. This is because Pt has larger spin as well as orbital contributions to its Knight shift than Pd in that concentration range.

Comparing the theoretical and experimental results for Ag in the two alloy systems, one finds that the Knight shifts of Ag in the two alloy systems do not differ much for $x > 0.30$. Their large difference on the Ag-poor side is attributed to the influence of Pd on Ag in Ag_xPd_{1-x}, with its large Stoner-enhanced spin magnetization, being stronger than that of Pt on Ag in Ag_xPt_{1-x}.

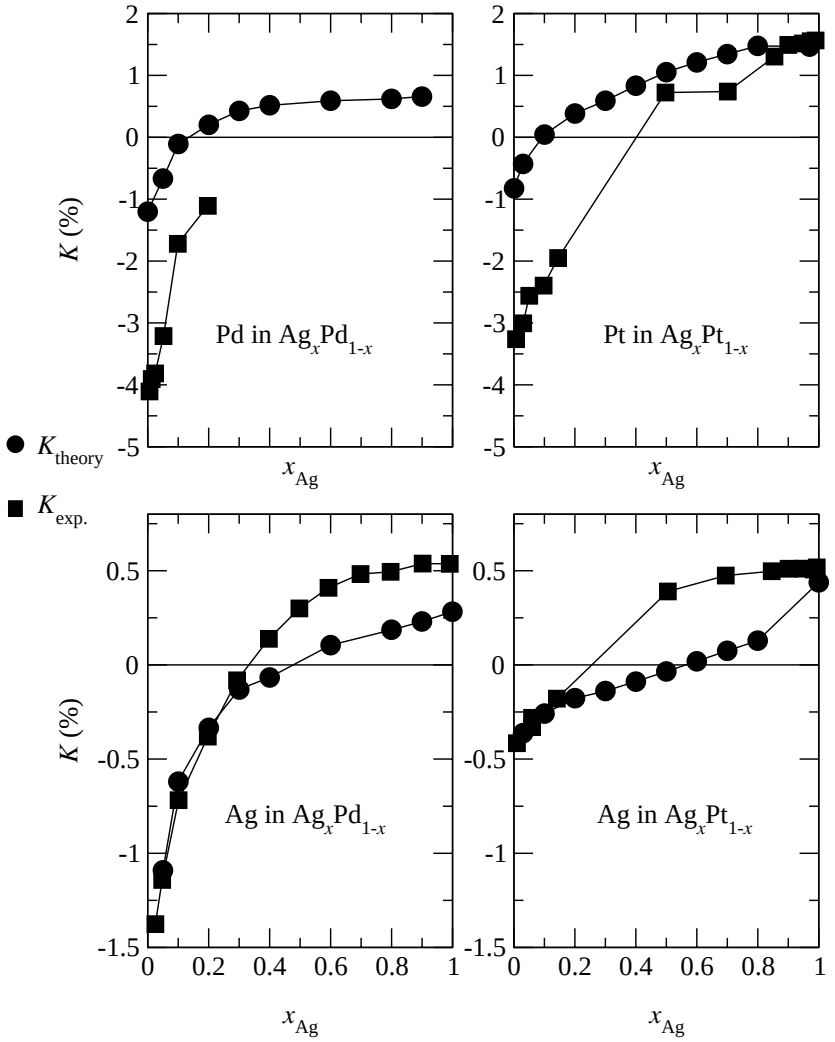

Figure 8. Calculated total Knight shifts of Ag and B in Ag_xB_{1-x} (B = Pd, Pt) in comparison with the experimental data [2, 14, 16, 44] .

For the Ag-poor side of the alloy systems one notes a rather pronounced deviation of the calculated Knight shifts of the alloy partners Pd and Pt from the corresponding experimental data. This has to be attributed to a large extent to problems in dealing with the core polarization mechanism within the framework of plain SDFT. The same problem is present when dealing with the corresponding core polarization hyperfine field in spontaneously magnetized solids which in general is also found to be too small compared with experiment. Recently, it became possible to demonstrate, using the so-called optimized potential method (OPM), that the core polarization hyperfine field is strongly increased compared with plain SDFT-type calculations, leading to a satisfying agreement with experiment [45]. From this, one can conclude that an improved treatment of the core polarization Knight shift K_{cp} should also improve the agreement with experiment in figure 8. Finally, it should be noted that there is always some ambiguity concerning the reference on which the experimental Knight shift is based [43].

Acknowledgments

This work was funded by the DFG (Deutsche Forschungsgemeinschaft) within the programme *Theorie relativistischer Effekte in der Chemie und Physik schwerer Elemente*.

References

[1] Terakura K, Hamada N, Oguchi T and Asada T 1982 *J. Phys. F: Met. Phys.* **12** 1661
[2] Narath A 1968 *J. Appl. Phys.* **39** 553
[3] Staunton J B 1982 *PhD Thesis* University of Bristol
[4] Matsumoto M, Staunton J B and Strange P 1990 *J. Phys.: Condens. Matter* **2** 8365
[5] Ebert H *et al* 1999 *Int. J. Quantum Chem.* **20** 1253
[6] Deng M, Freyer H and Ebert H 2000 *Solid State Commun.* **114** 365
[7] Benkowitsch J and Winter 1983 *J. Phys. F: Met. Phys.* **13** 991
[8] Brooks M S S 1985 *Physica* B **130** 6
[9] Ebert H and Battocletti M 1996 *Solid State Commun.* **98** 785
[10] Mott N F 1935 *Proc. Phys. Soc.* **47** 571
[11] Hoare F E, Matthews J C and Walling J C 1953 *Proc. R. Soc.* A **216** 502
[12] Montgomery H, Pells G P and Wray E M 1967 *Proc. R. Soc.* A **301** 261
[13] Brill P and Voitländer J 1975 *Z. Phys.* B **20** 369
[14] Gräf P, Ebert H, Akai H and Voitländer J 1993 *Hyperfine Interact.* **78** 1011
[15] Ebert H, Abart J and Voitländer J 1983 *J. Less-Common Met.* **91** 89
[16] Ebert H, Abart J and Voitländer J 1984 *J. Phys. F: Met. Phys.* **14** 749
[17] Kuentzler R *et al* 1988 *Z. Phys.* B **70** 357
[18] Staunton J B, Gyorffy B L and Weinberger P 1980 *J. Phys. F: Met. Phys.* **10** 2665
[19] Gyorffy B L and Stott M J 1973 *Band Structure Spectroscopy of Metals and Alloys* ed D J Fabian and L M Watson (New York: Academic) p 385
[20] Rose M E 1961 *Relativistic Electron Theory* (New York: Wiley)
[21] Gunnarsson O 1976 *J. Phys. F: Met. Phys.* **6** 587
[22] Mendelsohn L B, Biggs F and Mann J B 1970 *Phys. Rev.* A **2** 1130
[23] Yasui M and Shimizu M 1985 *J. Phys. F: Met. Phys.* **15** 2365
[24] Matsumoto M, Staunton J B and Strange P 1991 *J. Phys.: Condens. Matter* **3** 1453
[25] Durham P J, Gyorffy B L and Pindor A J 1980 *J. Phys. F: Met. Phys.* **10** 661
[26] Butler W H 1985 *Phys. Rev.* B **31** 3260
[27] Guo G Y, Temmerman W M and Ebert H 1991 *Physica* B **172** 61
[28] Shull C G and Ferrier R P 1963 *Phys. Rev. Lett.* **10** 295
[29] Stassis C, Kline G R and Sinha S K 1975 *Phys. Rev.* B **11** 2171
[30] Oh K H, Harmon B N, Liu S H and Sinha S K 1976 *Phys. Rev.* B **14** 1283
[31] Pindor A J, Temmerman W M, Gyorffy B L and Stocks G M 1980 *J. Phys. F: Met. Phys.* **10** 2617
[32] Winter H and Stocks G M 1983 *Phys. Rev.* B **27** 882
[33] Ebert H, Weinberger P and Voitländer J 1985 *Phys. Rev.* B **31** 7557
[34] Banhart J, Ebert H, Voitländer J and Winter H 1986 *J. Magn. Magn. Mater.* **61** 221
[35] Svensson B 1932 *Ann. Phys. Lpz.* **14** 699
[36] Jamieson H C and Manchester F D 1972 *J. Phys. F: Met. Phys.* **2** 323
[37] Kobayashi S, Asayama K and Itoh J 1963 *J. Phys. Soc. Japan* **18** 1735
[38] Narath A and Weaver H T 1971 *J. Physique Coll.* **32** C1 992
[39] Herberg H and Voitländer J 1980 *Phys. Rev.* B **22** 5043
[40] Krieger R and Voitländer J 1980 *Z. Phys.* B **40** 39
[41] Gyorffy B L 1973 *Band Structure Spectroscopy of Metals and Alloys* ed D J Fabian and L M Watson (New York: Academic) p 641
[42] Ebert H and Winter H 1987 *Solid State Commun.* **63** 899
[43] Carter G C, Bennett L H and Kahan D J 1977 *Prog. Mater. Sci.* **20** 153
[44] Ebert H 1981 *Diploma Thesis* University of Munich
[45] Akai H and Kotani T 1999 *Hyperfine Interact.* **120–121** 3